Since January 2020 Elsevier has created a COVID-19 resource centre with free information in English and Mandarin on the novel coronavirus COVID-19. The COVID-19 resource centre is hosted on Elsevier Connect, the company's public news and information website.

Journal of Theoretical Biology 454 (2018) 1–10

Contents lists available at ScienceDirect

Journal of Theoretical Biology

journal homepage: www.elsevier.com/locate/jtb

Modelling the skip-and-resurgence of Japanese encephalitis epidemics in Hong Kong

Shi Zhao, Yijun Lou, Alice P.Y. Chiu, Daihai He*

Department of Applied Mathematics, Hong Kong Polytechnic University, Hong Kong (SAR) China

ARTICLE INFO

Article history:
Received 12 October 2017
Revised 14 May 2018
Accepted 16 May 2018
Available online 21 May 2018

Keywords:
Japanese encephalitis virus
Mathematical modelling
Skip-and-resurgence
Vector-free transmission

ABSTRACT

Japanese encephalitis virus (JEV) is a zoonotic mosquito-borne virus, persisting in pigs, Ardeid birds and *Culex* mosquitoes. It is endemic to China and Southeastern Asia. The case-fatality ratio (CFR) or the rate of permanent psychiatric sequelae is 30% among symptomatic patients. There were no reported local JEV human cases between 2006 and 2010 in Hong Kong, but it was followed by a resurgence of cases from 2011 to 2017. The mechanism behind this "skip-and-resurgence" patterns is unclear.

This work aims to reveal the mechanism behind the "skip-and-resurgence" patterns using mathematical modelling and likelihood-based inference techniques. We found that pig-to-pig transmission increases the size of JEV epidemics but is unlikely to maintain the same level of transmission among pigs. The disappearance of JEV human cases in 2006–2010 could be explained by a sudden reduction of the population of farm pigs as a result of the implementation of the voluntary "pig-rearing licence surrendering" policy. The resurgence could be explained by of a new strain in 2011, which increased the transmissibility of the virus or the spill-over ratio from reservoir to host or both.

1. Introduction

Japanese encephalitis virus (JEV) is a zoonotic and mosquito-borne virus that is the major cause of viral encephalitis in Asia. The annual total confirmed human cases has decreased substantially from 12,594 cases to 3429 cases between 2006 and 2012, and then resurged to 5399 in 2016 (Fig. 1). The case-fatality ratio and the rate of permanent neurologic or psychiatric sequelae of patients with encephalitis can be 30% (Arai et al., 2008; Centers for Disease Control, 2017; Centers for Disease Control and Prevention, 2017; Libraty et al., 2002; Mackenzie et al., 2004; Solomon and Winter, 2004; World Health Organization, 2017; Lam et al., 2005) and over 35% in children (Kumar et al., 1990). JEV persists in a transmission cycle of pigs, Ardeid birds and mosquitoes. It could infect humans through mosquito bites by *Culex tritaeniorhynchus* species (Centers for Disease Control and Prevention, 2017; Center for Health Protection, 2017; World Health Organization, 2017). Humans are dead-end hosts where they cannot develop viremia to infect mosquitoes. Population sizes of farm pigs and the size of rice land, which favors the *Culex* mosquitoes' growth, are the two key factors affecting local transmission (Centers for Disease Control and Prevention, 2017; Impoinvil et al., 2018; World Health Organization, 2017).

Vertical transmission of JEV in mosquitoes and pig-to-pig transmission are the major determinants of the following year's transmission. Vertical transmission exists between mosquitoes and their e.g. Rosen et al. (1989, 1978); Takashima and Rosen (1989). Mosquito population increases during spring, peaks in summer and decreases during fall annually (Riley et al., 2007, 2012). According to a recent study by Ricklin et al., pig-to-pig transmission is also present (Ricklin et al., 2016a).

JEV transmission via blood transfusion has recently been found in Hong Kong, which was probably the first case worldwide. The transmission was reported to come from an asymptomatic viremic donor to two hospitalized patients (South China Morning Post, 2017).

Sero-prevalence of JEV antibodies varied by season among swines and among human population groups in Hong Kong. During rainy season between May and July, the sero-prevalence among swines reached 91% compared with 34% that is reported in dry season (Scientific Committee on Vector-borne Diseases, 2017). It was approximately 80%–90% among swines in July and August from 2000 to 2004 (Riley et al., 2007). Another local serological survey found that 23.5% of pig farmers and 5.9% of abattoir workers are seropositive to JEV antibodies, in contrast to 0% reported among 30 blood donors (Scientific Committee on Vector-borne Diseases, 2017).

JEV vaccine protection rates has been investigated. The vaccine was reported to have a high effective protection rate of 93.3% by

* Corresponding author.
E-mail address: daihai.he@polyu.edu.hk (D. He).

https://doi.org/10.1016/j.jtbi.2018.05.017
0022-5193/

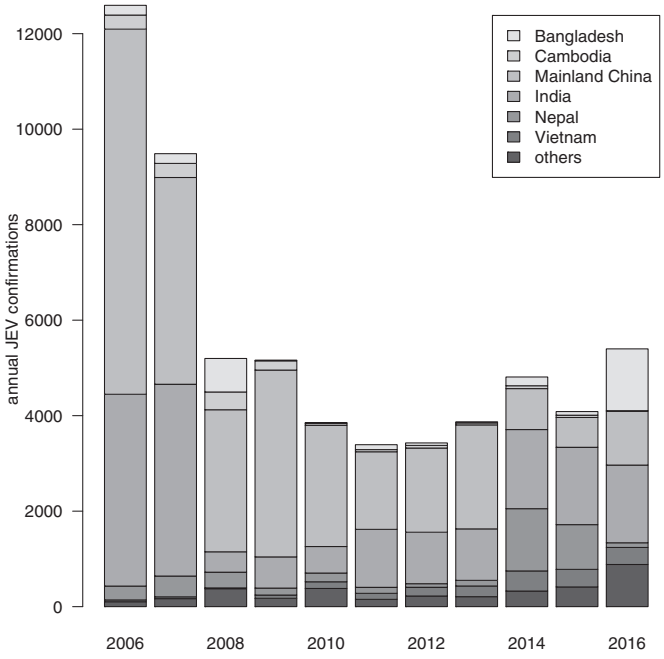

Fig. 1. Annual JEV confirmations from 2006 to 2016 among the top six JEV endemic countries and the total of other countries. Data are obtained from World Health Organization (2018).

five years and a predicted protection rate of 85.5% by 10 years (Desai et al., 2012). A recent study by Cao et al. investigated the current JEV vaccine derived from G3 JEV genotype against the emerging G5 genotype in mice, and found that the lethal challenge protection rate was 50%. The same study also reported that neutralizing antibodies against G5 JEV were detected in 35% of vaccinated healthy children (Cao et al., 2016).

Riley et al. examined the skip-and-resurgence patterns of JEV from 1969 to 2004 in Hong Kong (Riley et al., 2007). They suggested that the skip from 1990 to 2002, except for one case reported in 1996, was likely due to the lack of rice production, as *Culex* species breed principally in rice fields (Tian et al., 2015). They proposed that the resurgence from 2003 to 2004 was likely due to the heightening of infectious disease notification system after the Severe Acute Respiratory Syndrome (i.e., SARS) outbreak in 2003 in Hong Kong (Riley et al., 2007).

In Hong Kong, no locally-acquired JEV case was reported between 2006 and 2010, but 17 cases were reported between 2011 and June, 2017. Considering the declining local live pig population from 350,000 to 60,000 between 2004 and 2017 (Hong Kong, 2017; Legislative Council of Hong Kong, 2017a; 2017b; The Government of Hong Kong, Agriculture, Fisheries and Conservation Department, 2017a; 2017c), the disappearance of local JEV cases between 2006 and 2010 are expected, but the resurgence of local cases is intriguing.

Our work aims to identify the mechanism underlying the JEV skip-and-resurgence patterns between December 2003 and May 2017 in Hong Kong. We hypothesized such behavior could be due to the surrendering of pig licenses during a pig rearing policy change in 2006 and/or a new JEV strain invasion around 2011. These hypotheses are tested using mathematical modelling and likelihood-based inference techniques.

2. Data and methods

2.1. Data

The monthly JEV cases between December 2003 and May 2017 were retrieved online from the Centre for Health Protection in Hong Kong (Scientific Committee on Vector-borne Diseases, 2017; The Government of Hong Kong, Center for Health Protection, 2017). The regional monthly mosquito ovitrap index from December 2003 to December 2016 were retrieved online from the Food and Environmental Hygiene Department in Hong Kong (The Government of Hong Kong, Food and Environmental Hygiene Department, 2017). The annual pattern of reported JEV cases and regional mosquito ovitrap index are shown in Fig. 2. We present the time series of JEV cases and regional mosquito ovitrap index in Fig. 3.

The population sizes of live pigs in Hong Kong (Fig. 4) were obtained from local government reports, local news articles, and reports from Department of Agriculture in the United States (Hong Kong, 2017; Legislative Council of Hong Kong, 2017a; 2017b; Ta Kung Pao, 2017; The Government of Hong Kong, Agriculture, Fisheries and Conservation Department, 2017a; 2017c; FEHD, 2017a; 2017b; United States Department of Agriculture, 2017). Since the pig rearing license surrendering policy was implemented in May 2006, the number of local live pigs has rapidly declined. 243 out of 265 pig farms owners had surrendered their licenses (Legislative Council of Hong Kong, 2017b).

2.2. JEV compartmental model

Ricklin et al. recently reported that pig-to-pig transmission of JEV can also occur without the mosquito vectors (Ricklin et al., 2016a). After the infectious period in pigs where JEV in swine serum are infectious to mosquitoes, there is also a convalescent period in which pig sheds JEV virus in their oronasal secretions. Thus, the pig population could be classified into five compartments: susceptible, exposed, infectious, convalescent and recovered which are denoted as S_p, E_p, I_p, C_p and R_p respectively. We considered pig-to-pig transmission and vector-borne transmission. Fig. 5 shows the model diagram considering pigs, mosquitoes and humans. JEV transmission can be described by the following system of equations (Eq. (1)).

$$\begin{cases} S_p' = (1-\eta)\cdot B_p(t)\cdot N_p - \nu_p S_p - \left(\lambda_{vp} + \beta_p \cdot \frac{C_p}{N_p}\right) S_p, \\ E_p' = \left(\lambda_{vp} + \beta_p \cdot \frac{C_p}{N_p}\right) S_p - (\sigma_p + \nu_p) E_p, \\ I_p' = \eta \cdot B_p(t)\cdot N_p + \sigma_p E_p - (\gamma_p + \nu_p) I_p, \\ C_p' = \gamma_p I_p - (\delta_p + \nu_p) C_p, \\ R_p' = \delta_p C_p - \nu_p R_p. \end{cases} \tag{1}$$

Table 1 summarizes the model parameters in Eq. (1). The effects of $B_p(t)$ and ν_p are presented in the dynamics of local live pig population because $N_p' = [B_p(t) - \nu_p]N_p$. In this model, the total pig population is:

$$N_p = S_p + E_p + I_p + C_p + R_p,$$

where N_p is the observed live pig populations in Hong Kong and is a time-dependent parameter (see purple dashed line in Fig. 4). $B_p(t)$ is the time-dependent birth rate of local live pigs. Humans are dead-end hosts and cannot further transmit the disease (Centers for Disease Control and Prevention, 2017; Impoinvil et al., 2018; World Health Organization, 2017), thus we model human cases using a variable spill-over ratio (ρ) in week i ρ_i (see Eq. (2)):

$$Z_i = \int_{\text{week } i} \rho_i \gamma_p I_p \, dt. \tag{2}$$

Please see S.2.2 for more reasoning on model structure.

2.3. Model framework

JEV cases were modelled as a Partially Observed Markov Process (POMP), also known as Hidden Markov model, using R pack-

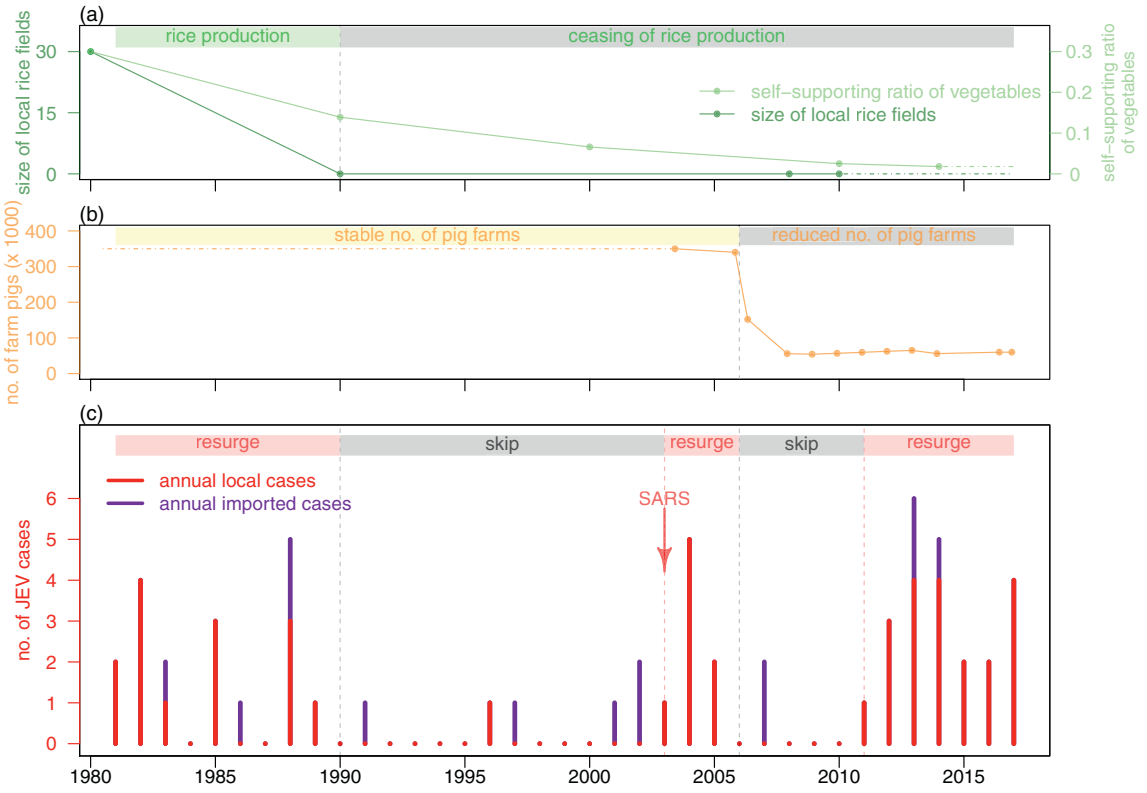

Fig. 2. Skip-and-resurgence of JEV epidemic from 1980 to 2017 in Hong Kong. Panel **(a)** shows the area of local rice production and self-supporting vegetable ratio. Panel **(b)** the orange line shows the number of local live pigs. Panel **(c)** shows the reported annual (i.e. both local and imported) JEV cases in Hong Kong. The arrow indicates the timing of SARS outbreak. (For interpretation of the references to color in this figure legend, the reader is referred to the web version of this article.)

Table 1
Model input parameters. We denote JEV transmitted from vectors to pigs as "v → p", and from pigs to humans as "p → h" respectively. Please see S.2.1 for more information of the initial proportions.

Parameters	Notations	Values	Ranges	Remarks/Units	Sources
Force of infection	λ_{vp}	-	time-dependent	v → p, per year	Eq. (3)
Latent period in pigs	σ_p^{-1}	1.5	1–2	days	Kodama et al. (1968); Ricklin et al. (2016a)
Infection period in pigs	γ_p^{-1}	3	2–4	days	Centers for Disease Control (2017); Kodama et al. (1968); Ricklin et al. (2016a,b); Williams et al. (2001)
Convalescent period in pigs	δ_p^{-1}	2.5	1–4	days	Ricklin et al. (2016a)
Proportion of infected among imported pigs	η	1.0%	0.43%–1.45%	pigs, Nil	Eq. (8)
Effective contact rate	β_p	estimate	0.0–0.4	pigs, per days	Eq. (10)
Lifespan of pigs	ν_p^{-1}	234.0	234.0	days	Eq. (7)
Population size of pigs	N_p	-	time-dependent	see Fig. 4	Hong Kong (2017); Legislative Council of Hong Kong (2017a,b); Scientific Committee on Vector-borne Diseases (2017); The Government of Hong Kong, Agriculture, Fisheries and Conservation Department (2017a,c)
Spill-over ratio	ρ	-	time-dependent	p → h, Nil	Eq. (5)
Initial proportion of susceptible	S_{p0}	estimate	45–75%	Nil	Center for Health Protection (2017); Konno (1969); Riley et al. (2007)
Initial proportion of exposed	E_{p0}	0.1%	–	Nil	assumed
Initial proportion of infectious	I_{p0}	0.1%	–	Nil	assumed
Initial proportion of convalescent	C_{p0}	0.1%	–	Nil	assumed
Initial proportion of recovered	R_{p0}	estimate	25–55%	Nil	Center for Health Protection (2017); Konno (1969); Riley et al. (2007)

age "POMP" (King, 2017). The iterated filtering and plug-and-play likelihood-based inference frameworks were employed to fit the time series (Gao et al., 2016; He et al., 2010; King et al., 2016). Furthermore, the Maximum Likelihood Estimate (MLE) was used to estimate the model parameters. To quantify the tradeoff between the goodness-of-fit of a model and its complexity (Schwarz, 1978), Bayesian Information Criterion (BIC) was used for model comparison. Simulations were performed by implementing the Euler-multinomial integration method with a fixed time-step of one day (Allen et al., 2008; He et al., 2010).

The model was first validated with the observed JEV cases in Hong Kong, based on information about the size of pig popula-

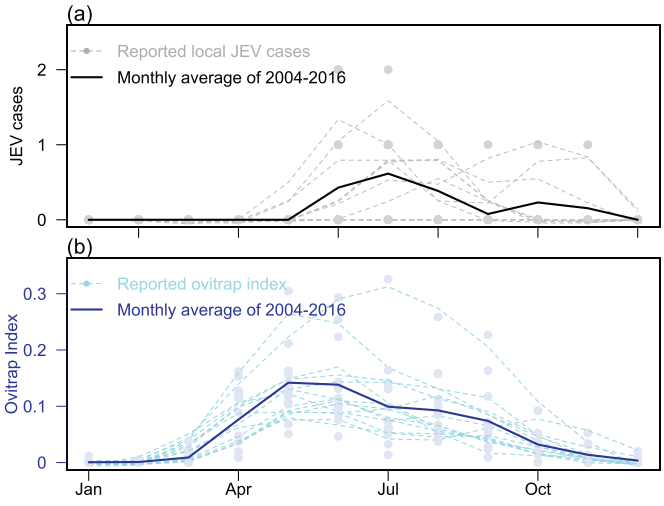

Fig. 3. Panel **(a)** shows the monthly reported local JEV cases in Hong Kong, and panel **(b)** shows the average monthly ovitrap index of regions (i.e., including Yuen Kong, Yuen Long and Tin Shui Wai) around Yuen Long district in Hong Kong. For both panels, darker lines represent annual averages, lighter lines represent smoothed data. Dots represent the annual reported data from 2004 to 2016.

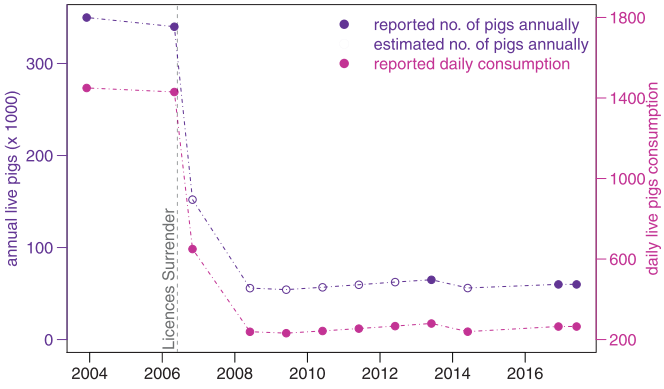

Fig. 4. Local live pig populations and their daily consumptions from January 2004 to May 2017 in Hong Kong. Purple line represents the annual live pig populations, connected by their reported and estimated numbers, which are depicted in filled and hollow circles respectively (N_p). Violet red line and dots represent the daily local live pig consumptions ($\nu_p N_p$). Vertical grey dashed line denotes the time when the pig rearing license surrendering policy was implemented in Hong Kong. (For interpretation of the references to color in this figure legend, the reader is referred to the web version of this article.)

tion. Mosquito abundance is a time-dependent parameter, which was smoothed over time based on the ovitrap index (ω). The force of infection (λ_{vp}) from vectors to reservoirs is another time-dependent parameter. The spill-over ratio (ρ) is estimated through ω.

The monthly observed cases, C_i, were assumed to follow a Poisson distribution (Poi), with a mean Z_i, the underlying monthly cases modelled by Eq. (2). Hence, we have:

$$C_i \sim \text{Poi}(\lambda = Z_i) \qquad \text{with} \quad \text{mean} : \mu_i = Z_i.$$

Thus, the overall log-likelihood function, l, was given by:

$$l(\Theta|C_1, \ldots, C_n) = \sum_{i=1}^{n} \ln f(C_i|C_{1:(i-1)}, \Theta)$$

where Θ denotes the parameter vector being estimated, $f(C_i|C_{1:(i-1)}, \Theta)$ was the posterior probability measurement function for C_i given $C_{1:(i-1)}$, which were then numerically computed by Sequential Monte Carlo (SMC, also known as particle filtering) (He et al., 2010), and n denotes the total number of months during the study period.

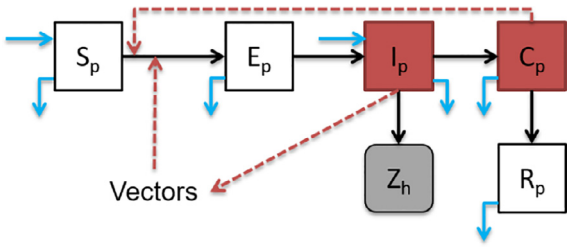

Fig. 5. JEV model diagram. Infectious classes are denoted in red, and JEV human cases are in grey (i.e., Z_h, or Z_i in Eq. (2)). The transition paths are represented in black arrows. Red dashed arrows represent paths of transmission. Births and deaths (including slaughtering) of pigs are represented in light blue arrows. (For interpretation of the references to color in this figure legend, the reader is referred to the web version of this article.)

Using the profile likelihood method, the confidence intervals (C.I.) of the model output parameters were estimated based on the model input parameter ranges as described in Table 1. Parameters estimation and statistical analyses are conducted using R (version 3.4.1) (R, 2018).

2.4. Parameter estimation

2.4.1. Force of infection from vectors to reservoirs (λ_{vp})

We can express λ_{vp} as $\lambda_{vp} = a\vartheta_{vp} \cdot \frac{I_v}{N_p}$, where a is the mosquito biting rate; ϑ_{vp} is the transmission probability of JEV per mosquito bite; and I_v is the number of infected mosquitoes. However, in this study, we simplify λ_{vp} as a function of ovitrap index over time, since we are employing a vector-free modelling framework. This is justifiable by assuming that a and ϑ_{vp} are constant, while $\frac{I_v}{N_p}$ is roughly proportional to the ovitrap index. Briefly, we assume:

$$\lambda_{vp} = k \cdot \omega(t) + b \tag{3}$$

where ω is the time series of ovitrap index in Hong Kong, k and b are model parameters under estimation. Constant b represents the contribution of the vertical transmission from adult mosquitoes to their eggs. The vertical transmission ratio of *Culex tritaeniorhynchus* is varied from 12% to nearly 100% (Rosen et al., 1989; Takashima and Rosen, 1989). By using Eq. (3), we also incorporate the case that despite the ovitrap index is close to zero during a dry season, the transmission rate can still be positive due to vertical transmission of vectors.

To investigate the mechanism of the observed resurgence of JEV after 2011 in Hong Kong, we partitioned the force of infection into time segments based on the hypothesis that the re-emergence was due to the invasion of a new JEV strain. This hypothesis is then validated using statistical approaches. We assume the force of infection (λ_{vp}) takes the following form:

$$\lambda_{vp} = \begin{cases} k_1 \cdot \omega(t) + b, & t < T_0 \\ k_2 \cdot \omega(t) + b, & t \geqslant T_0 \end{cases} \tag{4}$$

where T_0 is the time when the new JEV strain invaded.

Biologically, the force of infection (λ_{vp}) under the new strain invasion scenario is higher than the no-invasion scenario, since the pig population is immunologically naive in the first few years after invasion. Thus, under the new-strain invasion hypothesis, we have $k_2 > k_1 > 0$. The average spill-over ratio $\langle\lambda_{vp}\rangle$ after invasion should be much higher than that before invasion. Without new strain invasion, we have the special case where $k_1 = k_2$ in Eq. (4).

2.4.2. Spill-over ratio from reservoirs to humans (ρ)

In Eq. (2), we assume that humans are dead-end hosts (Centers for Disease Control and Prevention, 2017; Impoinvil et al., 2018; World Health Organization, 2017). Thus, the reported JEV human

cases are proportional to pig infections according to the time-dependent spill-over ratio(ρ). Since the number of human cases are related to the total number of vectors, we can further assume the spill-over ratio as a function of ovitrap index:

$$\rho = \xi \cdot \omega(t-\tau) \tag{5}$$

where ξ is the strength of infectivity parameter under estimation and τ is the sum of incubation period of mosquitoes (i.e. 6–12 days) (Konno, 1969; Takashima and Rosen, 1989; Van den Hurk et al., 2009), latent period in humans (i.e. 5–13 days) (Centers for Disease Control, 2017; Centers for Disease Control and Prevention, 2017; Center for Health Protection, 2017) and case-reporting delay. For simplicity, we fix τ to be 15 days for this study.

To investigate the mechanism of the observed resurgence of JEV after 2011 in Hong Kong, we partitioned the spill-over ratio into time segments based on the hypothesis that the re-emergence was due to the invasion of a new JEV strain. This hypothesis is then validated using statistical approaches. We assume the spill-over ratio (ρ) takes the following form from Tien et al. (2010):

$$\rho = \begin{cases} \xi_1 \cdot \omega(t-\tau), & t < T_0 \\ \xi_2 \cdot \omega(t-\tau), & t \geqslant T_0 \end{cases} \tag{6}$$

where T_0 is the time when the new JEV strain invaded.

Biologically, the spill-over ratio (ρ) under the new strain invasion scenario is much higher than the no-invasion scenario, since the pig population is immunologically naive in the first few years after invasion. Thus, under the new-strain invasion hypothesis, we have $\xi_2 > \xi_1 > 0$. The average spill-over ratio $\langle\rho\rangle$ after invasion should be much higher than that before invasion. Without new strain invasion, we have the special case where $\xi_1 = \xi_2$ in Eq. (6).

2.4.3. Lifespan of pigs (ν_p^{-1})

Hong Kong people consumed approximately 265 live domestic pigs per day during 2016–17 (FEHD, 2017a; 2017b), and roughly 275 live domestic pigs per day in around 2012 (Ta Kung Pao, 2017), whereas the consumption was around 1450 live domestic pigs back in 2004 (Legislative Council of Hong Kong, 2017b). The total pig population has fallen from 350,000 in 2004–05 (Legislative Council of Hong Kong, 2017a; 2017b; The Government of Hong Kong, Agriculture, Fisheries and Conservation Department, 2017c), to 65,000 in 2012 (The Government of Hong Kong, Agriculture, Fisheries and Conservation Department, 2017a) and further dropped to 60,000 in 2016–17 (Hong Kong, 2017). Thus the average lifespan of pigs $\langle\nu_p^{-1}\rangle$ can be estimated as:

$$\begin{aligned}
\text{During 2004-05}: \quad \langle\nu_p^{-1}\rangle &= \frac{N_p}{\text{daily consumptions}} \\
&= \frac{350000}{1450} \approx 241.38 \quad \text{days}, \\
\text{In 2012}: \quad \langle\nu_p^{-1}\rangle &= \frac{N_p}{\text{daily consumptions}} \\
&= \frac{65000}{275} \approx 236.36 \quad \text{days}, \\
\text{During 2016-17}: \quad \langle\nu_p^{-1}\rangle &= \frac{N_p}{\text{daily consumptions}} \\
&= \frac{60000}{265} \approx 226.42 \quad \text{days}.
\end{aligned} \tag{7}$$

By averaging the above, we computed the average lifespan of pigs ν_p^{-1} to be approximately 234 days.

2.4.4. Pigs' population (N_p)

Given that the average local living pig consumption is 650 live pigs per day in 2007 (Legislative Council of Hong Kong, 2017b), we approximate the total number of pigs (N_p) to be $234 \times 650 = 152,100$. The sudden drop in the number of live pigs between 2006 and 2007 was due to the surrendering of pig rearing licenses in early 2006, which result in 243 out of 265 pig farm owners turning over their licenses (Legislative Council of Hong Kong, 2017b). Although the daily live pig consumption is not included as a modelling parameter, given the pig's average lifespan, we could infer the total number of live pigs from the amount of daily consumption.

2.4.5. Infection ratio among imported pigs (η)

η can be computed as:

$$\eta = \langle \text{IAR}_p \rangle \cdot \frac{\gamma_p^{-1} + \delta_p^{-1}}{\langle \nu_p^{-1} \rangle}, \tag{8}$$

where $\langle \text{IAR}_p \rangle$ is the average attack rate over the average lifespan of pigs $\langle \nu_p^{-1} \rangle$. According to the value of parameter in Table 1, if γ_p^{-1} is 1.5 day, δ_p^{-1} is 2.5 days, $\langle \nu_p^{-1} \rangle$ is 234 days and $\langle \text{IAR}_p \rangle \in [25\%, 85\%]$ (Center for Health Protection, 2017; Khan et al., 2014), we estimated that $\eta \in [0.43\%, 1.45\%]$.

3. Results

3.1. Model fitting results

In addition to the simulated median, we also present the simulated annual means of the model prediction using the approach described in Camacho et al. (2014), since simulated means demonstrated fitting results more consistently when the data are being restricted as integers and are subject to stochastic noise.

The model fitting results under the new JEV strain invasion scenario are shown in Fig. 6. The estimated model parameters are summarized in Table 2. Although the long-term fitting suffers from severe stochastic noise (i.e. zero, one or two cases per month), the 95% simulated quantile interval covers all observed data, and the simulated average annual pattern is consistent with the observed pattern.

BIC reduces more than 28 units when we went from the baseline (i.e. no invasion, see S.1.1) scenario to the new strain invasion scenario (see Fig. 6 and explanation **I3** in Table 3). We modelled another new strain invasion scenario where only the force of infection λ_{vp} is partitioned (see explanation **I2** in Table 3 and S.1.3). The BIC increases approximately 1.0 unit which implies an almost equivalent fitting performance to the main results (see Fig. 6 and explanation **I3** in Table 3). The partitioned force of infection with no partition on spill-over ratio is presented in S.1.3 (see explanation **I2** in Table 3). Another invasion scenario with time-dependent λ_{vp} and ρ are investigated in S.1.2 (see explanation **I1** in Table 3), and BIC increases 4.55 unit. The detailed model performance and explanation of are in Table 3 and Supplementary Information.

3.2. Basic reproduction number of pig-to-pig transmission

Using the next generation matrix method (Brauer et al., 2016; Van den Driessche and Watmough, 2002), the basic reproduction number, $\mathcal{R}_{pp}$, of pig-to-pig transmission is computed as:

$$\mathcal{R}_{pp} = \frac{\beta_p \gamma_p \cdot (\eta \nu_p + \sigma_p)}{[(1-\eta)(\gamma_p + \delta_p + \nu_p)\nu_p + \gamma_p \delta_p](\nu_p + \sigma_p)}. \tag{9}$$

We consider that imported infections are rare ($\eta \approx 0^+$), and both incubation period and infection period of JEV in pigs are negligible (i.e., $\sigma_p^{-1} \approx 0^+$ and $\gamma_p^{-1} \approx 0^+$). Then, it could be seen that $\mathcal{R}_{pp} \approx \frac{\beta_p}{\delta_p + \nu_p}$, which is consistent with the standard SIR compartmental model (Allen et al., 2008). We estimated $\mathcal{R}_{pp}$ to be 0.0013 (95% C.I.: [0.00,0.31]) under the invasion scenario (see Fig. 7). Furthermore, the range of effective contact rate,

$$\beta_p \in [0.0, 0.4], \tag{10}$$

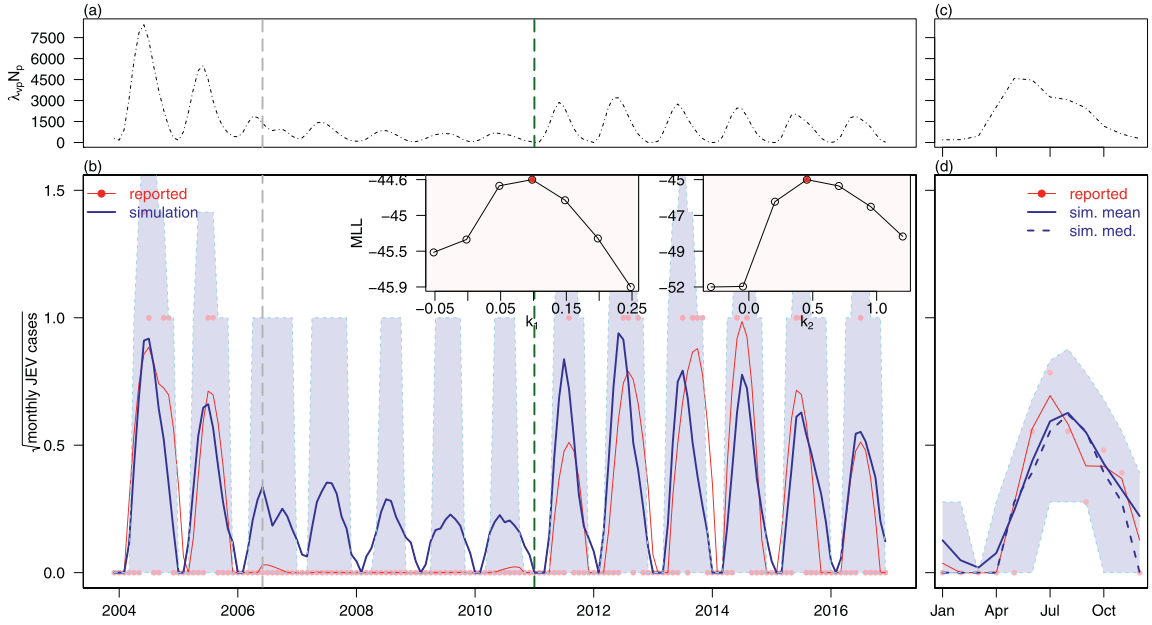

Fig. 6. Model fitting results of JEV local cases in Hong Kong from 2004 to 2016 under new JEV strain invasion scenario with variable ρ. Panel (a) and (b) are the scaled force of infection (from vectors to pigs, scaled by the population size of pigs) and simulation results from 2004 to 2016 respectively. Panel (c) and (d) are the one-year-average scaled force of infection and simulation results from 2004 to 2016 respectively. In panel (a) and (b), black dashed lines are the scaled force of infection. In panel (b) and (d), blue lines are the simulation results, shaded regions are 95% quantile interval from simulation, pink dots are the reported (i.e., observed) JEV local cases and red lines are the smoothed (by *loess* function) reported JEV cases. The vertical grey dashed line marks the time point when Hong Kong government triggered the pig rearing licences surrender policy. The vertical dark green dashed line marks the time point when the new JEV strain introduced to the pigs' population. The inset panel shows the maximum log-likelihood (MLL) values of different k_1s and k_2s , the red dot with the highest MLL are selected for fitting in main panels. The model scenario is associated with explanation **I3** in Table 3. (For interpretation of the references to color in this figure legend, the reader is referred to the web version of this article.)

Table 2
Summary table of model parameters' estimates under new JEV strain invasion scenario with both variable λ_{vp} and ρ. X_{p0} denotes the initial proportion of class X_p.

Parameter	Notation	Value	Type	Initial status	Unit/Remarks
Average force of infection	2004–10:$\langle\lambda_{vp}\rangle$	0.0043	estimated	time-dependent	before invasion
Average force of infection	2011–16:$\langle\lambda_{vp}\rangle$	0.0071	estimated	time-dependent	after invasion
Pig latent period	σ_p^{-1}	1.5	fixed	1–2	days
Pig infection period	γ_p^{-1}	3	fixed	2–4	days
Pig convalescent period	δ_p^{-1}	2.5	fixed	1–4	days
Imported infection ratio	η	1.0%	fixed	0.43%-1.45%	Nil
Effective contact rate	β_p	0.0058	estimated	0.0-0.4	per days
Pig living period	ν_p^{-1}	234	fixed	234	days
Pig population	N_p	–	–	time-dependent	pigs
Average spill over ratio	2004–10:$\langle\rho\rangle$	0.0002	estimated	time-dependent	before invasion
Average spill over ratio	2011-16:$\langle\rho\rangle$	0.0013	estimated	time-dependent	after invasion
Average ovitrap index	$\langle\omega\rangle$	0.0564	given	time-dependent	Nil
Initial susceptible	S_{p0}	0.6470	estimated	45–75%	Nil
Initial exposed	E_{p0}	0.001	assumed	0.0-0.25%	Nil
Initial infectious	I_{p0}	0.001	assumed	0.0-0.25%	Nil
Initial convalescent	C_{p0}	0.001	assumed	0.0-0.25%	Nil
Initial recovered	R_{p0}	0.3400	estimated	25–55%	Nil
BIC	BIC	144.8174	estimated	–	Nil

(see Tables 1 and 2) is set corresponding to $\mathcal{R}_{pp} \in [0.0, 1.0]$.

The range of $\mathcal{R}_{pp}$ could be inferred as follows: JEV sero-positive rates among pigs quickly decreases in winter (Riley et al., 2007). Mosquito abundance is almost zero during the same time period. Thus, this indicates the vector-free transmission of JEV among pigs cannot persist. Therefore, $\mathcal{R}_{pp}$ is less 1.0 and positive (i.e., greater than 0).

3.3. Critical community size

The critical community size (CCS) is defined as "*the minimum size of a closed population within which a host-to-host, non-zoonotic pathogen can persist indefinitely*" (Bartlett, 1960). Nåsell (2005) presented a method of approximating the CCS from simple compartmental models of directly-transmitted diseases. This is relevant to our study concerning pig-to-pig transmission. CCS can be formulated (obtained from Eq. (12.1) in Nåsell, 2005) as:

$$\mathrm{CCS} \approx \frac{2\pi}{\ln 2} \cdot \frac{\mathcal{R}_0 \cdot \alpha_p^{1.5}}{(\mathcal{R}_0 - 1)^{1.5}}, \tag{11}$$

where $\alpha_p = \frac{\gamma_p + \nu_p}{\nu_p}$ denotes the ratio of average lifespan of pigs (ν_p^{-1}) to the average duration of infection. The basic reproduction number of pig-to-pig transmission, $\mathcal{R}_{pp}$ in Eq. (9) is relatively small compared to that of vector-borne transmission, $\mathcal{R}_{vp}$. A modelling study by Khan et al. estimated $\mathcal{R}_{vp}$ to be 1.2 among pigs (Khan et al., 2014). Also, $\mathcal{R}_{vp}$ is believed to be greater than 1.0, as JEV does spread during every rainy season. Applying the parameters under the new strain invasion scenario in Table 2

Table 3
Summary of model fitting results and associated trait(s) under different scenarios.

Label	Scenario and its trait(s)	BIC	△BIC[a]	Remarks
B	baseline (no invasion)	168.7009	28.4376	see S.1.1
I1	invasion (ρ changed since 2011)	140.2633	0.0	see S.1.2
I2	invasion (λ_{vp} changed since 2011)	141.2743	1.0110	see S.1.3
I3	invasion (ρ and λ_{vp} changed since 2011)	144.8174	4.5541	see Fig. 6 and Table 2

[a] $\triangle BIC = BIC - BIC_{min}$, where BIC_{min} is the minimum of BICs of all scenarios. Here, $BIC_{min} = 140.2633$ (see S.1.2).

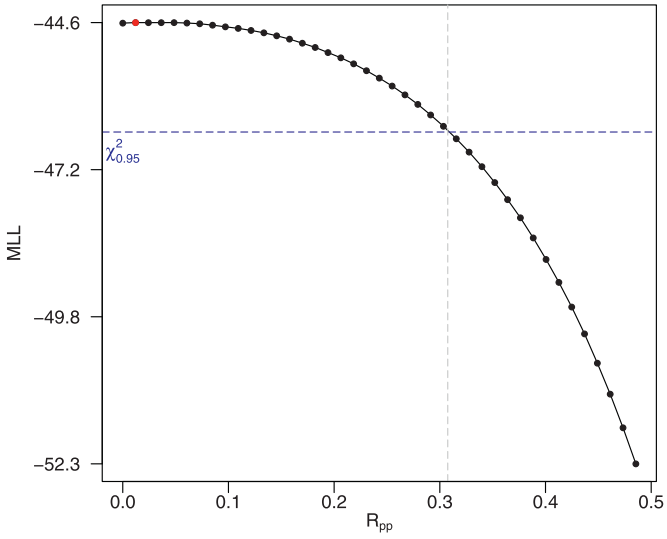

Fig. 7. The results of estimation of the basic reproduction number of pig-to-pig transmission ($\mathcal{R}_{pp}$) under new JEV strain invasion scenario with variable ρ. The horizontal blue dashed line is the 95% confidence threshold. The model scenario is associated with explanation **I3** in Table 3. (For interpretation of the references to color in this figure legend, the reader is referred to the web version of this article.)

(explanation **I3** in Table 3) to Eq. (9), $\mathcal{R}_{pp}$ is merely 0.0013, which is much smaller than $\mathcal{R}_{vp}$. By using the next generation matrix approach (Brauer et al., 2016; Gao et al., 2016), the basic reproduction number is:

$$\mathcal{R}_0 = \frac{\mathcal{R}_{pp} + \sqrt{\mathcal{R}_{pp}^2 + 4\mathcal{R}_{vp}^2}}{2}.$$

If we ignore the effects of $\mathcal{R}_{pp}$ (i.e., $\mathcal{R}_{pp} \approx 0^+$ as in Gao et al., 2016), we have $\mathcal{R}_0 \approx \mathcal{R}_{vp}$. If we fix $\nu_p^{-1} = 234.0$ (see Eq. (7)), and set $\mathcal{R}_0 \in [1.10, 1.40]$ and $\gamma_p^{-1} \in [2.0, 4.0]$ (thus, $\alpha_p \in [59.5, 118.0]$), the relationship among α_p, $\mathcal{R}_0$ and CCS (in Eq. (11)) are illustrated in Fig. 8.

The number of local live pigs was reduced from 80,000 to 60,000 since 2008 after the pig license surrendering policy came into effect (Fig. 4) (Legislative Council of Hong Kong, 2017b). With relatively low $\mathcal{R}_0$, CCS is greater than 150,000 (see the area below the blue line in Fig. 8) over a broad range of α_p's. This could explain the local JEV case disappearance from 2006 to 2010 in Hong Kong.

Moreover, for the invasion scenario, we found that the force of infection, λ_{vp}, could increase after the introduction of new JEV strain while assuming a fixed spill-over ratio, ρ. The fitting results of the partitioned force of infection, which did not partition on the spill-over ratio, are presented in the S.1.3 (see explanation **I2** in Table 3). The goodness-of-fit is almost equivalent to the previous scenario. We modelled the partitioned λ_{vp} and ρ scenario in S.1.2 (see explanation **I1** in Table 3). Although the fitting results are not as good as in the invasion scenario,(i.e. the main results in Fig. 6 and explanation **I3** in Table 3), it is still a significant improvement from the baseline (no invasion) scenario. The estimated force of infection, λ_{vp}, also increases after introducing a new JEV strain (see S.1.2 and explanation **I1** in Table 3). With an increased $\mathcal{R}_0$ due to an increased λ_{vp}, the CCS level could become lower than the local live pig's population level (see Fig. 8), which explains the resurgence of JEV cases. Further discussion on $\mathcal{R}_0$ and CCS can be found in S.2.3

4. Discussion

In this study, we argue that the resurgence of JEV after 2011 was likely due to new strain invasion that has a higher transmissibility. some indirect overseas evidence does exist: (i) **JEV genotype 1 (G1) strain since 2000:** In Southeast Asia, studies reported that Genotype 3 was predominant during the late 20th century, and then genotype 1 started to replace genotype 3 around 2000 and become dominant thereafter (Gao et al., 2015; Mackenzie et al., 2004; Pan et al., 2011). One genetic study found that the genotype 1 strain was not observed until 2008 in the regions of Mainland China surrounding Hong Kong (Gao et al., 2013). Thus, it is very likely that there is a newly introduced JEV strain from pigs imported from these Mainland Chinese regions (The Government of Hong Kong, Agriculture, Fisheries and Conservation Department, 2017b); (ii) **JEV genotype 5 (G5) strain:** Similar JEV resurgences were observed in South Korea in 1998 and 2010 (Sunwoo et al., 2016). The resurgence in 1998 was likely due to the introduction of G1 strain in the mid-1990's (Gao et al., 2013; Mackenzie et al., 2004). The first isolated local G5 strain was reported in 2010 in South Korea, which coincided with the resurgence of JEV in 2010 (Takhampunya et al., 2011), where the average number of annual JEV cases increased approximately six- to eight-fold (Sunwoo et al., 2016). This is also consistent with our results of explanation **I1** and **I3** in Table 3.

We achieved almost equivalent goodness-of-fit under the two invasion scenarios. There are three potential explanations for the JEV resurgence since 2011: (**I1**) The newly introduced JEV strain has slightly increased the transmissibility from vectors to pigs, and considerably increased the spill-over ratio from pigs to humans; (**I2**) The newly introduced JEV strain has considerably increased the transmissibility, but the spill-over ratio is held constant; (**I3**) The main results: the newly introduced JEV strain has increased both the transmissibility and the spill-over ratio. Please also see the summary of **I1**-**I3** in Table 3.

The symptomatic ratio of JEV could be further used to refine the mathematical model. As the majority of JEV infections are asymptomatic, and the mortality ratio for clinical JEV cases are approximately 30% (Table 4). We assume the symptomatic ratio of JEV among pigs are the same as that of humans, and asymptomatic pigs have negligible JEV transmissibility to vectors due to low within-host viral loads.

Our main results are derived from **I3** (Fig. 6). In Table 2, we estimated the annual force of infection $\langle \lambda_{vp} \rangle$ to be 0.0042 and the proportion of susceptible pigs S_{p0} to be 68% at the beginning of each year (Center for Health Protection, 2017; Konno, 1969; Riley et al., 2007), the annual average JEV infection attack rate (IAR_p)

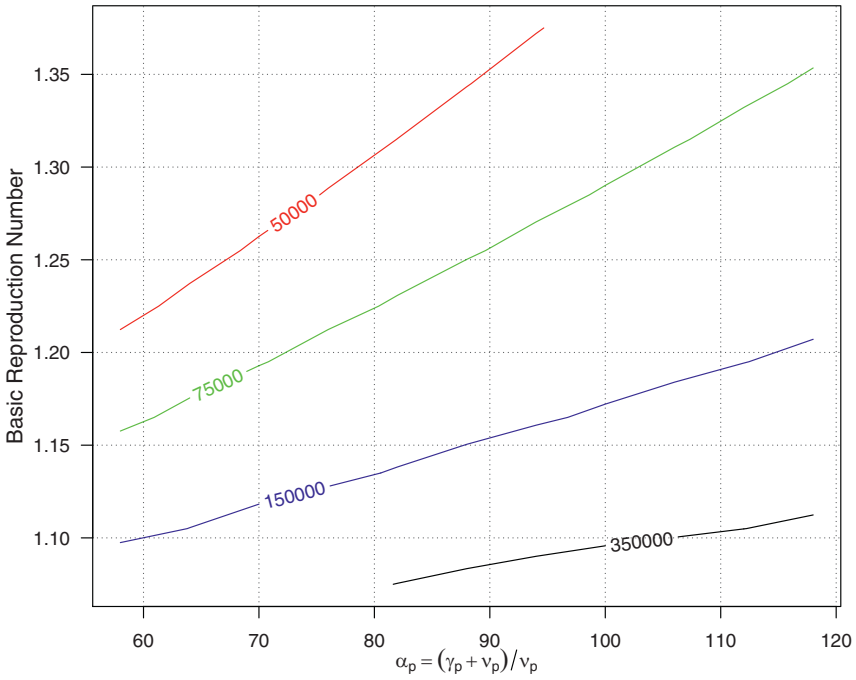

Fig. 8. Contour plot of the relationships between critical community size (CCS), α_p and the basic reproduction number $\mathcal{R}_0$. Numbers indicating the different CCS levels.

Table 4
Symptomatic JEV infection ratio and case-fatality ratio (CFR) of JEV with clinical illness from various sources. The numbers in brackets are the geometric average of the upper and lower ranges.

$\frac{\text{Symptomatics}}{\text{Total Infections}}$ (Symptomatic%)	CFR = $\frac{\text{Mortality}}{\text{Clinical Illness}}$	Source(s)
(0.48%) 0.4%–0.5%	30%	Centers for Disease Control (2017); World Health Organization (2017)
< 1%	20%–30%	Arai et al. (2008); Centers for Disease Control and Prevention (2017)
(0.81%) 0.33%–2%	25%	Libraty et al. (2002)
(0.63%) 0.1%–4%	25%–30%	Mackenzie et al. (2004); Solomon and Winter (2004)
4% (occasionally)	–	Van den Hurk et al. (2009)
(0.63%) 0.1%-4%	–	Chakraborty et al. (1980); Grossman et al. (1973, 1973); Halstead and Grosz (1962); Konishi and Suzuki (2002)
–	35%	Monath et al. (2000)
–	36.4% (children)	Kumar et al. (1990)

among pigs could be computed as

$$\text{IAR}_p = \frac{\langle \lambda_{vp} \rangle \cdot S_{p0}}{\text{Symptomatic\%}}$$

where Symptomatic% is the JEV symptomatic rate, by which IAR_p is estimated from 35.26% to 59.50% (with Symptomatic% $\in$ [0.48%, 0.81%]), which is consistent with (Center for Health Protection, 2017; Khan et al., 2014; Riley et al., 2007). The results corresponding to **I2** are presented in S.1.3, where the annual transmission rate $\langle \lambda_{vp} \rangle$ is set to be 0.0044 and 0.1763 before and after invasion, respectively. The larger annual force of infection after invasion produces unreasonable IAR_p. With parameter values in S.1.3, $\langle \lambda_{vp} \rangle = 0.1763$ and $S_{p0} = 57.67\%$ lead to $\text{IAR}_p \in [1255\%, 2118\%]$, which is larger than 100%. The mechanism **I3** implies increase in both λ_{vp} and ρ after invasion (see S.1.2). With $S_{p0} = 64\%$, IAR_p is increased from [33.98%,57.33%] to [56.10%, 94.67%] after invasion, within acceptable ranges. Therefore, according to the range of IAR_p, **I1** and **I3** are likely to be the possible explanations of the resurgence of JEV epidemics in 2011, while **I2** is unlikely since it predicts unreasonable values of IAR_p.

Furthermore, **I3** could be more biologically reasonable than **I1**. In **I1**, we assumed the force of infection (i.e., λ_{vp}) unchanged but only change the value of spill-over rate before/after the new JEV invasion. However, with the force of infection in **I1**, the JEV epidemic is unlike to maintain according to the estimation results of CCS (i.e., in this case, the pig population is lower than the CCS). On the contrary, with increased force of infection in **I3**, the JEV epidemic is very likely to come back (i.e., resurgent) since 2011. Further work is needed in order to identify the biological evidences and mechanisms of **I3**.

In this work, we only investigated the scenarios of new JEV invasion, more possible causes (or scenarios) due to various other factors can be further explored.

5. Conclusions

We developed a simple mathematical model to investigate the mechanisms behind the skip-and-resurgence patterns of JEV human cases in Hong Kong. The critical community size (CCS) estimated through the model indicates that the pig rearing license surrender policy on May 2006 could be responsible for the disappearance of JEV human during 2006–10, assuming that other factors remain unchanged. Compared with the results of baseline (no invasion) scenario (see S.1.1), our fitting results in the hypothetical scenario imply that the resurgence of JEV in 2011 was likely due to the introduction of new strains which has a higher transmissibility and/or a spill-over ratio.

The basic reproduction number ($\mathcal{R}_{pp}$) of pig-to-pig transmission is estimated to be 0.0013 (95% C.I.: [0.00,0.30]). Although the vector-free JEV transmission route exists (Ricklin et al., 2016a) and it could increase the epidemic size and prolongs the outbreak, JEV is unable to spread among pigs without vectors.

Thus vector control remains the most important and effective measure in mitigating JEV outbreaks in Hong Kong. Apparently, the reduction in local farm pig did not lead to elimination of JEV in Hong Kong. But monitoring JEV among pigs is still very important. This work shed light on the understanding of JEV epidemic in the other parts of Asia.

Acknowledgments

The model simulations are performed on workstations of the Department of Applied Mathematics at the Hong Kong Polytechnic University. This work was partially supported by the Early Career Schemes (PolyU 251001/14M and PolyU 253004/14P) and General Research Fund (PolyU 153277/16P) from Hong Kong Research Grants Council.

Supplementary material

Supplementary material associated with this article can be found, in the online version, at 10.1016/j.jtbi.2018.05.017.

References

Allen, L.J., Brauer, F., Van den Driessche, P., Wu, J., 2008. Mathematical epidemiology. Lect. Notes Math. 1945, 81–130.
Arai, S., Matsunaga, Y., Takasaki, T., Tanaka-Taya, K., Taniguchi, K., Okabe, N., Kurane, I., 2008. Vaccine preventable diseases surveillance program of japan. Japanese encephalitis: surveillance and elimination effort in Japan from 1982 to 2004. Jpn. J. Infect. Dis. 61 (5), 333–338.
Bartlett, M.S., 1960. The critical community size for measles in the United States. J. R. Stat. Soc. Ser. A (Gen.) 37–44.
Brauer, F., Castillo-Chavez, C., Mubayi, A., Towers, S., 2016. Some models for epidemics of vector-transmitted diseases. Infect. Dis. Model. 1 (1), 79–87.
Camacho, A., Kucharski, A.J., Funk, S., Breman, J., Piot, P., Edmunds, W.J., 2014. Potential for large outbreaks of Ebola virus disease. Epidemics 9 70–8.
Cao, L., Fu, S., Gao, X., Li, M., Cui, S., Li, X., Cao, Y., Lei, W., Lu, Z., He, Y., Wang, H., 2016. Low protective efficacy of the current japanese encephalitis vaccine against the emerging genotype 5 Japanese encephalitis virus. PLoS Negl. Trop. Dis. 10 (5), e0004686.
Centers for Disease Control, R.O.C. (Taiwan), 2017. Japanese encephalitis. http://www.cdc.gov.tw/english/info.aspx?treeid=E79C7A9E1E9B1CDF&nowtreeid=E02C24F0DACDD729&tid=784CF7F674BD5DFA. Accessed on July.
Centers for Disease Control and Prevention (CDC), 2017. Japanese encephalitis. https://www.cdc.gov/japaneseencephalitis/index.html. Accessed on July.
Center for Health Protection, 2017. Japanese encephalitis. http://www.chp.gov.hk/en/content/9/24/28.html. Accessed on July.
Chakraborty, M.S., Chakravarti, S.K., Mukherjee, K.K., Mitra, A.C., 1980. Inapparent infection by Japanese encephalitis (JE) virus in West Bengal. Indian J. Pub. Health 24 (3) 121–7.
Desai, K., Coudeville, L., Bailleux, F., 2012. Modelling the long-term persistence of neutralizing antibody in adults after one dose of live attenuated Japanese encephalitis chimeric virus vaccine. Vaccine 30 (15), 2510–2515.
Gao, D., Lou, Y., He, D., Porco, T.C., Kuang, Y., Chowell, G., et al., 2016. Prevention and control of Zika as a mosquito-borne and sexually transmitted disease: a mathematical modeling analysis. Sci. Rep. 6, 28070.
Gao, X., Liu, H., Li, M., Fu, S., Liang, G., 2015. Insights into the evolutionary history of Japanese encephalitis virus (JEV) based on whole-genome sequences comprising the five genotypes. Virol. J. 12 (1), 43.
Gao, X., Liu, H., Wang, H., Fu, S., Guo, Z., Liang, G., 2013. Southernmost Asia is the source of Japanese encephalitis virus (genotype 1) diversity from which the viruses disperse and evolve throughout Asia. PLoS Negl. Trop. Dis. 7 (9), e2459.
Grossman, R.A., Edelman, R., Chiewanich, P., Voodhikul, P., Siriwan, C., 1973. Study of Japanese encephalitis virus in Chiangmai Valley, Thailand. II. Human clinical infections. Am. J. Epidemiol. 98, 121–132.
Grossman, R.A., Edelman, R., Willhight, M., Pantuwatana, S., Udomsakdi, S., 1973. Study of Japanese encephalitis virus in Chiangmai Valley, Thailand: III. Human seroepidemiology and inapparent infections. Am. J. Epidemiol. 98 (2), 133–149.
Halstead, S.B., Grosz, C.R., 1962. Subclinical Japanese encephalitis I. Infection of Americans with limited residence in Korea. Am. J. Hyg. 75 (2), 190–201.
He, D., Ionides, E.L., King, A.A., 2010. Plug-and-play inference for disease dynamics: measles in large and small populations as a case study. J. R. Soc. Interface 7 271–83.
Hong Kong 01, 2017. Press release. (URL). Accessed on August.
Impoinvil, D.E., Baylis, M., Solomon, T., 2018. Japanese encephalitis: on the one health agenda. One Health: The Human-Animal-Environment Interfaces in Emerging Infectious Diseases The Concept and Examples of a One Health Approach (Current Topics in Microbiology and Immunology, 365). Springer Berlin Heidelberg : Imprint: Springer, Berlin, Heidelberg.
Khan, S.U., Salje, H., Hannan, A., Islam, M.A., Bhuyan, A.M., Islam, M.A., Rahman, M.Z., Nahar, N., Hossain, M.J., Luby, S.P., Gurley, E.S., 2014. Dynamics of Japanese encephalitis virus transmission among pigs in northwest Bangladesh and the potential impact of pig vaccination. PLoS Negl. Trop. Dis. 8 (9), e3166.
King, A. A., 2017. Statistical inference for partially-observed Markov processes. In: http://www.kingaa.github.io/pomp/; accessed on June.
King, A.A., Nguyen, D., Ionides, E.L., 2016. Statistical inference for partially observed Markov processes via the R package pomp. J. Stat. Softw. 69, 1–43.
Kodama, K., Sasaki, N., Inoue, Y.K., 1968. Studies of live attenuated Japanese encephalitis vaccine in swine. J. Immunol. 100 (1), 194–200.
Konishi, E., Suzuki, T., 2002. Ratios of subclinical to clinical Japanese encephalitis (JE) virus infections in vaccinated populations: evaluation of an inactivated JE vaccine by comparing the ratios with those in unvaccinated populations. Vaccine 21 (1), 98–107.
Konno, J., 1969. Cyclic outbreak of Japanese encephalitis among pigs and humans. Jpn. J. Trop. Med. 10 (2), 132–133.
Kumar, R., Mathur, A., Kumar, A., Sharma, S., Chakraborty, S., Chaturvedi, U.C., 1990. Clinical features & prognostic indicators of Japanese encephalitis in children in Lucknow (India). Indian J. Med. Res. 91, 321–327.
Lam, K., Tsang, O.T., Yung, R.W., Lau, K.K., 2005. Japanese encephalitis in Hong Hong. Hong Kong Med. J. 11 (3), 182–188.
Legislative Council of Hong Kong, 2017a. Official Report (CB(2) 1663/05-06(05)). (URL)Accessed on August.
Legislative Council of Hong Kong, 2017b. Official Report (CB(2)2445/06-07(01)). (URL). Accessed on August.
Libraty, D.H., Nisalak, A., Endy, T.P., Suntayakorn, S., Vaughn, D.W., Innis, B.L., 2002. Clinical and immunological risk factors for severe disease in Japanese encephalitis. Trans. R. Soc. Trop. Med. Hyg. 96 (2), 173–178.
Mackenzie, J.S., Gubler, D.J., Petersen, L.R., 2004. Emerging flaviviruses: the spread and resurgence of Japanese encephalitis, West Nile and dengue viruses. Nat. Med. 10, S98–109.
Monath, T.P., Levenbook, I., Soike, K., Zhang, Z.X., Ratterree, M., Draper, K., Barrett, A.D., Nichols, R., Weltzin, R., Arroyo, J., Guirakhoo, F., 2000. Chimeric yellow fever virus 17D-Japanese encephalitis virus vaccine: dose-response effectiveness and extended safety testing in rhesus monkeys. J. Virol. 74 (4) 1742–51.
Nåsell, I., 2005. A new look at the critical community size for childhood infections. Theor. Popul. Biol. 67 (3), 203–216.
Pan, X.L., Liu, H., Wang, H.Y., Fu, S.H., Liu, H.Z., Zhang, H.L., Li, M.H., Gao, X.Y., Wang, J.L., Sun, X.H., Lu, X.J., 2011. Emergence of genotype I of Japanese encephalitis virus as the dominant genotype in Asia. J. Virol. 85 (19), 9847–9853.
R, 2018. The R project for statistical computing. https://www.r-project.org/.
Ricklin, M.E., Garcia-Nicolas, O., Brechbuhl, D., Python, S., Zumkehr, B., Nougairede, A., Charrel, R.N., Posthaus, H., Oevermann, A., Summerfield, A., 2016. Vector-free transmission and persistence of Japanese encephalitis virus in pigs. Nat. Commun. 7.
Ricklin, M.E., Garcia-Nicolas, O., Brechbuhl, D., Python, S., Zumkehr, B., Posthaus, H., Oevermann, A., Summerfield, A., 2016. Japanese encephalitis virus tropism in experimentally infected pigs. Vet. Res. 47 (1), 34.
Riley, S., Leung, G.M., Ho, L.M., Cowling, B.J., 2007. Identification of the key elements of transmission of Japanese encephalitis virus in hong kong. RFCID 05050132.
Riley, S., Leung, G.M., Ho, L.M., Cowling, B.J., 2012. Transmission of Japanese encephalitis virus in Hong Kong. Hong Kong Med. J. 18 (Suppl. 2), 45–46.
Rosen, L., Lien, J.C., Shroyer, D.A., Baker, R.H., Lu, L.C., 1989. Experimental vertical transmission of Japanese encephalitis virus by Culex tritaeniorhynchus and other mosquitoes. Am. J. Trop. Med. Hyg. 40 (5), 548–556.
Rosen, L., Tesh, R.B., Lien, J.C., Cross, J.H., 1978. Transovarial transmission of Japanese encephalitis virus by mosquitoes. Science 199 (4331) 909–11.
Schwarz, G., 1978. Estimating the dimension of a model. Ann. Stat. 6 461–4.
Scientific Committee on Vector-borne Diseases, Hong Kong, 2017. Official website. http://www.chp.gov.hk/en/sas7/101/110/107.html. accessed on July.
Solomon, T., Winter, P.M., 2004. Neurovirulence and host factors in flavivirus encephalitis–evidence from clinical epidemiology. Arch. Virol. Suppl. (18) 161–170.
South China Morning Post Website, 2017. http://www.scmp.com/news/hong-kong/health-environment/article/2103667/hong-kong-tackles-worlds-first-case-patient. Accessed on August.
Sunwoo, J.S., Jung, K.H., Lee, S.T., Lee, S.K., Chu, K., 2016. Reemergence of Japanese encephalitis in South Korea, 2010!V2015. Emerg. Infect Dis. 22 (10), 1841.
Takashima, I., Rosen, L., 1989. Horizontal and vertical transmission of Japanese encephalitis virus by Aedes japonicus (Diptera: Culicidae). J. Med. Entomol. 26 (5) 454–8.
Takhampunya, R., Kim, H.C., Tippayachai, B., Kengluecha, A., Klein, T.A., Lee, W.J., Grieco, J., Evans, B.P., 2011. Emergence of Japanese encephalitis virus genotype Vin the Republic of Korea. Virol. J. 8 (1), 449.
Ta Kung Pao in Hong Kong, 2017. Press release. (URL). Accessed on August.
The Government of Hong Kong, Agriculture, Fisheries and Conservation Department (AFCD), 2017a. Annual reports. http://www.afcd.gov.hk/misc/download/annualreport2012/agriculture.html. Accessed on August.
The Government of Hong Kong, Agriculture, Fisheries and Conservation Department (AFCD), 2017b. Imported live pigs. https://www.afcd.gov.hk/English/quarantine/qua_ie/qua_ie_ipab/qua_ie_ipab_ilpbp/qua_ie_ipab_ilpbp.html; Accessed on August.
The Government of Hong Kong, Agriculture, Fisheries and Conservation Department (AFCD), 2017c. Official website. http://www.afcd.gov.hk/eindex.html. accessed on July.

The Government of Hong Kong, Center for Health Protection (CHP), 2017. Statistics on communicable diseases official website. http://www.chp.gov.hk/en/notifiable1/10/26/43.html. Accessed on July.

The Government of Hong Kong, Food and Environmental Hygiene Department, 2017. Pest control website. http://www.fehd.gov.hk/english/safefood/dengue_fever/index.html. Accessed on July.

The Government of Hong Kong, Food and Environmental Hygiene Department (FEHD), 2017a. Press release official website. http://www.sc.isd.gov.hk/gb/www.info.gov.hk/gia/general/201011/04/P201011040289.htmand http://www.fehd.gov.hk/english/index.html. Accessed on July.

The Government of Hong Kong, Food and Environmental Hygiene Department (FEHD), 2017b. Monthly average daily supply and auction prices of live pigs. http://www.fehd.gov.hk/tc_chi/sh/data/supply_avg_tw.html. Accessed on August.

Tian, H.Y., Bi, P., Cazelles, B., Zhou, S., Huang, S.Q., Yang, J., Pei, Y., Wu, X.X., Fu, S.H., Tong, S.L., Wang, H.Y., 2015. How environmental conditions impact mosquito ecology and Japanese encephalitis: an eco-epidemiological approach. Environ. Int. 79, 17–24.

Tien, J.H., Poinar, H.N., Fisman, D.N., Earn, D.J., 2010. Herald waves of cholera in nineteenth century London. J. R. Soc. Interface. rsif20100494

United States Department of Agriculture (USDA), 2017. Global Agriculture Information Network (GAIN) Reports. http://www.usfoods-hongkong.net/res/mns/00321/HK1330.pdf and http://www.usfoods-hongkong.net/res/mns/00433/HK1524.pdf. accessed on September.

Van den Driessche, P., Watmough, J., 2002. Reproduction numbers and sub-threshold endemic equilibria for compartmental models of disease transmission. Math. Biosci. 180 (1), 29–48.

Van den Hurk, A.F., Ritchie, S.A., Mackenzie, J.S., 2009. Ecology and geographical expansion of Japanese encephalitis virus. Annu. Rev. Entomol. 54, 17–35.

Williams, D.T., Daniels, P.W., Lunt, R.A., Wang, L.F., Newberry, K.M., Mackenzie, J.S., 2001. Experimental infections of pigs with Japanese encephalitis virus and closely related australian flaviviruses. Am. J. Trop. Med. Hyg. 65 (4), 379–387.

World Health Organization, 2017. Japanese encephalitis fact sheet. http://www.who.int/mediacentre/factsheets/fs386/en/. Accessed on July.

World Health Organization, 2018. Japanese encephalitis annual incidence record. http://www.apps.who.int/immunization_monitoring/globalsummary/timeseries/tsincidencejapenc.html. Accessed on April